

Non-equilibrium phase-transitions in multi-component Rydberg gases

D. S. Ding,^{1,2,*} C. S. Adams,^{3,†} B. S. Shi,^{1,2,‡} and G. C. Guo^{1,2}

¹Key Laboratory of Quantum Information, University of Science and Technology of China, Hefei, Anhui 230026, China.

²Synergetic Innovation Center of Quantum Information and Quantum Physics, University of Science and Technology of China, Hefei, Anhui 230026, China.

³Department of Physics, Joint Quantum Centre (JQC) Durham-Newcastle, Durham University, South Road, Durham DH1 3LE, United Kingdom

(Dated: October 10, 2018)

Highly-excited Rydberg atoms have strong long-range interactions resulting in exotic optical properties such as large single photon non-linearities and intrinsic bistability. In this paper we study optical-driven non-equilibrium phase transitions in a thermal Rydberg gas with a sensitivity two order of magnitude higher than in previous work. In this regime we can elucidate the effect of interactions on the bistable optical response, and exploit different branches in the potential in order to study multi-component Rydberg gases with a rich of phase diagram including overlapping bistable regions. In addition, we study the effect of polarization on the width of the hysteresis loop. Finally, we observe that the medium exhibits a dynamical instability resulting from the competing dynamics of excitation and decay.

PACS numbers: 42.65.Pc 32.80.Rm 42.62.Fi 64.60.Ht

Highly-excited Rydberg atoms have exaggerated atomic properties [1] offering enormous potential for applications in quantum information processing [2], quantum optics [3] and quantum many-body physics [4, 5]. Central to these phenomena is the dipole blockade mechanism [6], where one Rydberg excitation induces a change in the excitation energy of neighboring atoms. Continuous driving of an ensemble results in exotic non-equilibrium phenomena such as collective quantum jumps [7], and non-equilibrium phase transitions [8–10], leading to optical instability [10]. Non-equilibrium physics is particularly important because of its wider significance to other fields where most systems fall into this category. The degree of control offered by Rydberg atoms makes it a useful platform to explore analogies with more complex phenomena such as photosynthetic energy exchange [11, 12], and non-equilibrium dynamics in economics, ecosystems and climate [13].

Generally, it was thought that the observation of non-equilibrium phase transitions in a light-matter system required optical cavity feedback [14–16]; or the cooperative response from resonant dipole-dipole interactions [17] observed at cryogenic temperatures [18]. In contrast, Rydberg media offer direct observation of non-equilibrium phase transitions without cryogenics or cavity feedback [10]. In previous work the phase transition was detected either via population shelving or exciting state fluorescence. The limitations of these techniques is that the read-out depends on the population of the Rydberg state and generally the observed linewidths and lineshifts are quite large, of order a few hundred megahertz [10].

Here, we report on the direct detection of an optically driven non-equilibrium phase transition using electromagnetically induced transparency (EIT) [19, 20]. This has the advantage that we can achieve much narrower linewidths resulting in a sensitivity two orders of magni-

tude higher than in previous work [10]. In this regime we observe new phenomena such as multi-region bistability resulting from different branches in the interaction potential, polarization effects, and a new dynamical instability which depends on polarization of the light. As the theory of driven-dissipative non-equilibrium dynamics is extremely demanding, our results should provide important pointers for benchmarking of different theoretical approaches [21–24]. We show that a simple mean field model with both attractive and repulsive Rydberg dipole-dipole interactions can result in the observed double bistability, however, a more sophisticated analysis will be needed to explain the full range of phenomena observed.

Fig. 1 illustrates the experimental setup and level scheme. The probe laser excites ground state atoms in Rubidium 85, labelled $|g\rangle$ corresponding to the $5S_{1/2}(F=2)$ state, to an intermediate state $|e\rangle$, $5P_{1/2}(F=3)$, with a detuning Δ_p . The probe laser is split into two beams and one is overlapped with a counter-propagating coupling laser that is resonant with the transition from $|e\rangle$ to a Rydberg state $|r\rangle$, $nD_{3/2}$, such that the Doppler effect in the EIT spectra is reduced by a factor $-v(\omega_p - \omega_c)/c$, where v is the velocity of atoms, ω_p and ω_c denote the angular frequency of probe and coupling fields. The probe and coupling lasers have Rabi frequencies Ω_p and Ω_c , respectively.

The probe fields are focused into the center of the Rubidium 85 (^{85}Rb) vapor cell (~ 5 cm) with beam waists of $31 \mu\text{m}$. The temperature of cell is 50°C , corresponding to atomic density of $1.5 \times 10^{11} \text{ cm}^{-3}$. The coupling laser operating at 480 nm has a power of 750 mW and is focussed to a beam waist of $18 \mu\text{m}$. We obtain an EIT spectrum by detecting the probe light while scanning the frequency of coupling laser. We set the frequency of probe laser near-resonant with the $|g\rangle \rightarrow |e\rangle$ transition. By using another

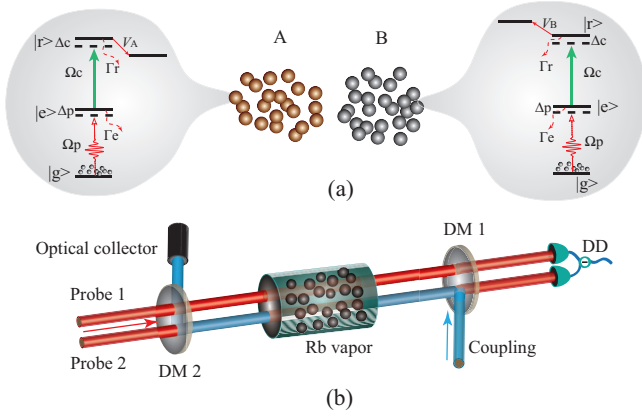


Figure 1. (a) Multi-component Rydberg gas with coupled species labeled as A and B, with atoms numbers of N_A and N_B ($N_A + N_B = N$). The diagram in the shadow box represents the energy level of each atomic species. The atomic levels including ground state $|g\rangle$, intermediate state $|e\rangle$ (decay rate Γ_e) and highly-excited Rydberg state $|r\rangle$ (decay rate Γ_r). The different interaction strengths in A and B components are V_A and V_B , which can have different signs. (b) Simplified experimental setup. DM: dichroic mirror, reflecting light at 475 nm and transmitting the 795 nm light. DD: differencing detector.

probe beam (probe 1) as a reference, we obtain an amplified differential probe of the transmission DD shown in Fig. 1(b). Typical spectra are shown in Fig. 2. We observe a much smaller linewidths than in previous work. For example in Fig. 2(d) we obtain a sensitivity of optical bistability of < 1 MHz comparing to a few hundred megahertz observed in Ref. [10].

Also immediately apparent in Fig. 2(a) is that we observe some new features in the spectra. In particular, there is a phase transition on both the red and the blue side of resonance, which can sit on top of one another when the probe is very weak as shown in Fig. 2(d). This near-resonance bistability displays extreme sensitivity to the phase transition.

The obvious question is whether this double bistability could arise to different branches in the interaction potential. As we are exciting D-state Rydberg atoms we know that the Rydberg level is degenerate and that the effect of interactions splits this degeneracy with states moving to both lower and higher energy. To model this effect we develop a mean-field which includes the different terms in the D-state interaction potential.

Considering of a system of N atoms continuously excited by a laser from the ground state to a Rydberg state. In order to model the different branches in the interaction potential we treat the gas as a mixture of two species with N_A and N_B atoms, $N_A + N_B = N$, as shown by Fig. 1(a). We note that this is an oversimplification as there are more than two components as we shall see later. The Hamiltonian for this two-component system, in the in-

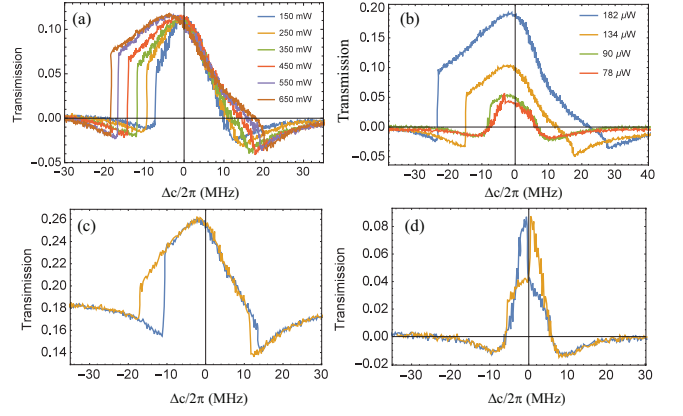


Figure 2. (a) The non-equilibrium phase transition appearing in both blue-detuning and red-detuning with a coupling laser power from 450 mW to 650 mW. In this case, the Rydberg principal number is 47. (b) The phase transitions observed with decreasing probe power. (c) The observed double non-equilibrium phase transitions while scanning the coupling detuning Δ_c from high-frequency to low-frequency (yellow line), and from low-frequency to high-frequency (blue line). The region of non-equilibrium phase transition appears near a red/blue-detuning of $\pm 2\pi \times 12.5$ MHz. (d) The abnormal non-equilibrium phase transition with weak probe beam (71 μ W). The red-detuned and blue-detuned regions are almost symmetric. The yellow and blue lines are scanned from high-frequency to low-frequency, and vice versa.

teraction picture, under rotating-wave approximation, is ($\hbar = 1$)

$$H = \sum_{i \in N_A} H_i + \sum_{j \in N_B} H_j + V_A \sum_{k \neq i, \in N_A} |r\rangle \langle r|_i \otimes |r\rangle \langle r|_k + V_B \sum_{k \neq j, \in N_B} |r\rangle \langle r|_j \otimes |r\rangle \langle r|_k \quad (1)$$

with

$$H_q = -\frac{1}{2}(\Omega_p |e\rangle \langle g|_q + \Omega_p |g\rangle \langle e|_q + \Omega_c |r\rangle \langle e|_q + \Omega_c |e\rangle \langle r|_q - 2\Delta_p |e\rangle \langle e|_q - 2\Delta_p |r\rangle \langle r|_q + 2\Delta_c |r\rangle \langle r|_q)$$

where q defines the q -th atom, with respective to the i -th and j -th atom in components A and B. The interaction strength V_A and V_B corresponds to attractive and repulsive branch in the full dipole-dipole interaction between D-states. To obtain an EIT lineshape for the two-component mixture we solve the master equation

$$\dot{\rho} = -i[H, \rho] + \sum_{i \in N_A} \mathcal{L}[\rho_i] + \sum_{j \in N_B} \mathcal{L}[\rho_j] \quad (2)$$

where the Lindblad operator $\mathcal{L}[\rho_m]$ ($m=i, j$) describes the decay of Rydberg states and the intermediate states of

single atom

$$\mathcal{L}[\rho_m] = \begin{pmatrix} \Gamma_e \rho_{m,ee} & -\frac{1}{2}\Gamma_e \rho_{m,ge} & -\frac{1}{2}\Gamma_r \rho_{m,gr} \\ -\frac{1}{2}\Gamma_e \rho_{m,eg} & -\Gamma_e \rho_{m,ee} + \Gamma_r \rho_{m,rr} & -\frac{1}{2}(\Gamma_r + \Gamma_e) \rho_{m,er} \\ -\frac{1}{2}\Gamma_r \rho_{m,rg} & -\frac{1}{2}(\Gamma_r + \Gamma_e) \rho_{m,rg} & -\Gamma_r \rho_{m,rr} \end{pmatrix} \quad (3)$$

We introduce a mean-field theory for each component A and B, via an effective detuning Δ_c of i -th and j -th atom are $\Delta_{c,i,eff} = \Delta_c - V_A \sum_k \rho_{k,rr}^A - \eta_1 V_B \sum_l \rho_{l,rr}^B$, $\Delta_{c,j,eff} = \Delta_c - V_A \sum_k \rho_{k,rr}^A - \eta_2 V_B \sum_l \rho_{l,rr}^B$, where $k \neq i$; $l \neq j$. We derive the steady-state solution for atomic density matrix for each group A and B, and obtain the roots of ρ_{eg}^A and ρ_{eg}^B , which characterize the absorption and dispersion for each component. The overall susceptibility is related to density matrix by

$$\chi^{A/B} = -\frac{2n_{A/B}\mu_{eg}^2}{\epsilon_0 \Omega_p} \rho_{eg}^{A/B} \quad (4)$$

where ϵ_0 is the permittivity of vacuum, μ_{eg} is the electric dipole matrix element related to the transition between levels $|e\rangle$ and $|g\rangle$. The absorption of probe laser beam is determined by $e^{-\text{Im}[\chi^A + \chi^B]kz/2}$, where the wavevector $k=2\pi/\lambda$.

The calculated transmission profile of the probe field is shown in Fig. 3. We see that there are regions of instability both above and below resonance which reproduces the observation of bistability on red- and blue-side of observed experimentally in Fig. 2. The two phase transitions are induced by the two components which were associated with negative and positive level shifts V_A and V_B , respectively. We can relate the negative and positive shifts back to the specific Rydberg states involved. The dipole-dipole energy shift is

$$\tilde{\Delta} = \Delta/2 - \text{sign}(\Delta) \sqrt{\Delta^2/4 + (\sqrt{D_\varphi} C_3/R^3)^2} \quad (5)$$

where Δ is the Förster energy mismatch, sign is the Signum function, $\sqrt{D_\varphi} C_3/R^3$ is the dipole-dipole interaction strength dependent on distance between Rydberg atoms, $\sqrt{D_\varphi}$ is the coefficient depending on angular (Clebsch-Gordan) coefficients [25]. In Rubidium, the dipole-dipole shift can be red- or blue-shifted when the D states strongly couple the F states [25]. Because the Förster channel $nD_{3/2} + nD_{3/2} \rightarrow n+1F_{5/2} + n-1F_{5/2}$ or $nD_{3/2} + nD_{3/2} \rightarrow n+2F_{5/2} + n-2F_{5/2}$ contribute to the positive energy shift, whilst another Förster channel $nD_{3/2} + nD_{3/2} \rightarrow n+1F_{5/2} + n+1F_{5/2}$ or $nD_{3/2} + nD_{3/2} \rightarrow n+2F_{5/2} + n+2F_{5/2}$ induce the negative energy shift.

Although, a simple two component steady-state mean-field model, Fig. 3, at least qualitatively accounts for the observed double bistability, it cannot account for the

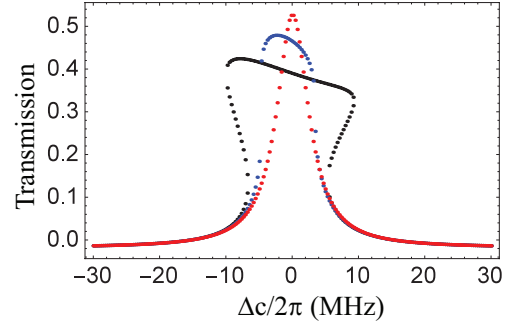


Figure 3. The theoretical simulated transmission of probe 2 field under the conditions of $\Omega_c=5.5 \Gamma$, $\Omega_p=2.5 \Gamma$, $\Gamma_r=0.5 \Gamma$, $\Gamma_e=6 \Gamma$, $\Delta_p=0$ with coupling coefficients $\eta_1=0.7$ and $\eta_2=1$. The spectra correspond to conditions of $V_A=-100 \Gamma$, $V_B=90 \Gamma$ (black); blue dots $V_A=-50 \Gamma$, $V_B=45 \Gamma$ (blue); and red dots $V_A=0 \Gamma$, $V_B=0 \Gamma$ (red) respectively.

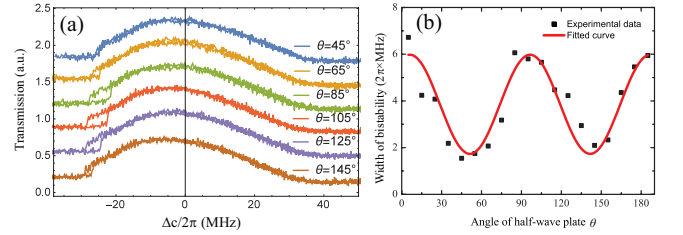


Figure 4. (a) The recorded spectra with different polarization of coupling beam. (b) The corresponding width of hysteresis loop against different polarized angles ($n=70$).

overlapping bistability of Fig. 2(d), and we also observe other phenomena which motivate a more sophisticated model of the full multi-component dynamics involving more than two states. Our detection methods allow us to exploit the polarization degree of freedom as the probe and couple beams may be either equally or orthogonally polarized. By varying the polarization we can investigate the effects of different magnetic sub-levels and the angular dependence of the interaction.

In Fig. 4 we show the effect of changing the polarization of the coupling beam when the Rydberg laser is tuned to a D-state with principle quantum number $n = 70$. The hysteresis loop closes when the polarizations of the probe and coupling fields become orthogonal. Fig. 4(b) shows the width of hysteresis loop as a function of the angle of the inserted half-wave plate, showing a dependence on the polarization angle between probe and coupling laser beams. This dependence is linked to different interaction strengths of hyperfine energy levels $nD_{3/2}$ ($m_j=3/2$) and $nD_{3/2}$ ($m_j=1/2$). The dipole-dipole interaction strength of $m_j=3/2$ is larger than $m_j=1/2$, which coincidentally results in different widths of the hysteresis.

When the hysteresis loop is nearly closed we observe the appearance of an optical instability (shown in Fig. 5(b)). The instability can be understood in

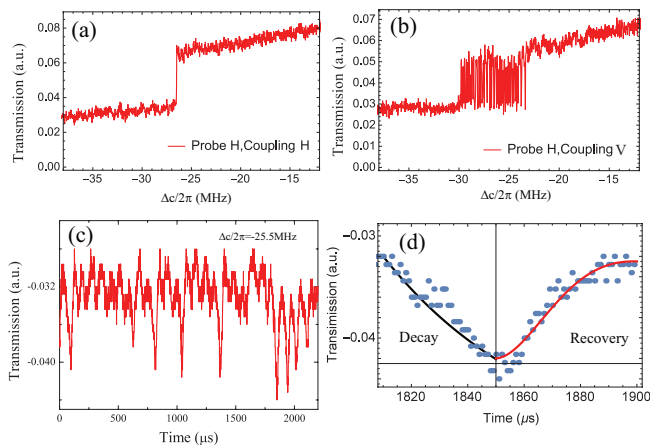


Figure 5. (a) Non-equilibrium phase transition when both probe and coupling laser have horizontal polarization. (b) An optical instability appears when the polarizations of the probe and coupling lasers are orthogonal. The power of probe and coupling laser beams are $150\mu\text{W}$ and 600mW , respectively. (c) The transmission of probe field when $\Delta_c \sim -2\pi \times 25.5\text{ MHz}$. (d) Details of the instability spike from (c), the black line corresponds to decay with $39\mu\text{s}$, and the red line to the recovery process due to driving.

terms of a competition between the multi-component non-equilibrium phases and population transfer between Zeeman sub-levels due to Larmor precession. The instability is sensitive to the fluctuations of the laser field, it tends to occur when the probe laser is frequency modulated, which suggests that the process needs a seed but there is not a deterministic relationship between the frequency modulation and the dynamics of the instability.

In order to characterize the time response of the system during the instability process we set the detuning to $\Delta_c \sim -2\pi \times 25.5\text{ MHz}$ and record the transmission spectrum verses time. There are many collective jumps in spectrum (Fig. 5(c)). The fourier spectrum contains white noise plus a component at the modulation frequency demonstrating the significance of the seed. The enlarged collective jump shown in Fig. 5(d) shows an exponential decay corresponding to a Rydberg lifetime of $29\mu\text{s}$, close to the expected lifetime of $70D_{3/2}$ Rydberg state at 320 K . We simulate the recovery process with Rabi frequency of 0.065 MHz , shown by red line in Fig. 5(d). These timescales give a useful impression of the natural response time of the medium.

In summary, we study experimentally an optically driven non-equilibrium phase transition in a Rydberg gas using EIT. In contrast to previous work based on a strong probe [10], we achieve a much higher frequency sensitivity and can observe coherent effects such as overlapping multi-component phase transitions. We observe a double hysteresis in agreement with a two-component static mean-field model. We also see a polarization dependence that relates to the angular dependence of the interaction

potentials, and the appearance of an optical instability. Our results highlight the rich range of non-equilibrium phenomena that are accessible in a relatively simple experiment, and provide observational data that is the key to benchmarking of theoretical models. Finally, the extreme sensitivity of non-equilibrium systems to small perturbation makes them very attractive for applications in sensing of, for example, microwave or terahertz fields. Our work contributes to the deeper understanding of the underlying physics which brings such application a step closer.

We are grateful to Min Xiao, Wei Yi for valuable discussions. We thank Jing Qian and Yan Li for help with theory and programming. This work was the National Natural Science Foundation of China (Grant Nos. 11174271, 61275115, 61435011, 61525504), and the Innovation Fund from CAS. CSA acknowledges financial support from EPSRC Grant Ref. No. EP/M014398/1, the EU RIA project ‘RYSQ’ project and DSTL.

* dds@ustc.edu.cn

† c.s.adams@durham.ac.uk

‡ drshi@ustc.edu.cn

- [1] T. F. Gallagher, *Rydberg atoms*, Vol. 3 (Cambridge University Press, 2005).
- [2] M. Saffman, arXiv preprint arXiv:1605.05207 (2016).
- [3] O. Firstenberg, C. S. Adams, and S. Hofferberth, arXiv preprint arXiv:1602.06117 (2016).
- [4] P. Schauß, M. Cheneau, M. Endres, T. Fukuhara, S. Hild, A. Omran, T. Pohl, C. Gross, S. Kuhr, and I. Bloch, *Nature* **491**, 87 (2012).
- [5] H. Labuhn, D. Barredo, S. Ravets, S. de Léséleuc, T. Macrì, T. Lahaye, and A. Browaeys, arXiv preprint arXiv:1509.04543 (2015).
- [6] M. Lukin, M. Fleischhauer, R. Cote, L. Duan, D. Jaksch, J. Cirac, and P. Zoller, *Physical Review Letters* **87**, 037901 (2001).
- [7] S. Diehl, A. Tomadin, A. Micheli, R. Fazio, and P. Zoller, *Physical review letters* **105**, 015702 (2010).
- [8] T. E. Lee, H. Häffner, and M. Cross, *Physical Review A* **84**, 031402 (2011).
- [9] J. Qian, L. Zhou, and W. Zhang, *Physical Review A* **87**, 063421 (2013).
- [10] C. Carr, R. Ritter, C. Wade, C. S. Adams, and K. J. Weatherill, *Physical review letters* **111**, 113901 (2013).
- [11] G. S. Engel, T. R. Calhoun, E. L. Read, T.-K. Ahn, T. Mančal, Y.-C. Cheng, R. E. Blankenship, and G. R. Fleming, *Nature* **446**, 782 (2007).
- [12] G. Panitchayangkoon, D. V. Voronine, D. Abramavicius, J. R. Caram, N. H. Lewis, S. Mukamel, and G. S. Engel, *Proceedings of the National Academy of Sciences* **108**, 20908 (2011).
- [13] H. Haken, *Naturwissenschaften* **67**, 121 (1980).
- [14] H. Gibbs, S. McCall, and T. Venkatesan, *Physical Review Letters* **36**, 1135 (1976).
- [15] H. Wang, D. Goorskey, and M. Xiao, *Physical Review A* **65**, 011801 (2001).
- [16] H. Wang, D. Goorskey, and M. Xiao, *Physical review*

- letters **87**, 073601 (2001).
- [17] H. Carmichael and D. Walls, *Journal of Physics B: Atomic and Molecular Physics* **10**, L685 (1977).
- [18] M. Hehlen, H. Güdel, Q. Shu, J. Rai, S. Rai, and S. Rand, *Physical review letters* **73**, 1103 (1994).
- [19] S. Harris, J. Field, and A. Imamoglu, *Physical Review Letters* **64**, 1107 (1990).
- [20] A. Mohapatra, T. Jackson, and C. Adams, *Physical review letters* **98**, 113003 (2007).
- [21] T. E. Lee, H. Haeffner, and M. Cross, *Physical review letters* **108**, 023602 (2012).
- [22] M. Marcuzzi, E. Levi, S. Diehl, J. P. Garrahan, and I. Lesanovsky, *Physical review letters* **113**, 210401 (2014).
- [23] H. Weimer, *Physical review letters* **114**, 040402 (2015).
- [24] N. Šibalić, C. G. Wade, C. S. Adams, K. J. Weatherill, and T. Pohl, *arXiv preprint arXiv:1512.02123* (2015).
- [25] T. G. Walker and M. Saffman, *Physical Review A* **77**, 032723 (2008).